

Zero-Field Splitting, Field-Dependent Magnetization of Mixed-Valent $S = 3/2$ Diruthenium(II,III) Tetracarboxylates

William W. Shum, Yi Liao, and Joel S. Miller*

Department of Chemistry, University of Utah, 315 South 1400 East Room 2124, Salt Lake City, Utah 84112-0850

Received: March 23, 2004; In Final Form: May 28, 2004

The 2 K field-dependent magnetization, $M(H)$, of $S = 3/2$ $[\text{Ru}^{\text{II/III}}_2(\text{OAc})_4]^+$ was studied. $[\text{Ru}^{\text{II/III}}_2(\text{OAc})_4]^+$ exhibits an unusually low magnetization with respect to that predicted by the classical Brillouin function. This reduced value is a consequence of the large anisotropy arising from the large zero-field splitting (ZFS), D ($+63 \pm 11 \text{ cm}^{-1}$), of the $[\text{Ru}^{\text{II/III}}_2(\text{OAc})_4]^+$ cation, which alters the energy levels with respect to the isotropic energy levels used to derive the Brillouin function. Analytical expressions for the parallel and perpendicular components of $M(H)$ that include zero-field splitting (ZFS), D , and interdimer coupling, θ , are presented for $S = 3/2$. The expression was derived from second-order perturbation theory for $|D| \gg g\mu_B H$. The experimental data fit very well with $g = 2.24 \pm 0.01$, $D = +69.5 \text{ cm}^{-1}$ ($D/k_B = +100 \text{ K}$), and $0 > \theta > -0.6 \text{ K}$ indicative of very weak interdimer interactions for both $[\text{Ru}^{\text{II/III}}_2(\text{OAc})_4]\text{Cl}$ and $[\text{Ru}^{\text{II/III}}_2(\text{OAc})_4]_3[\text{Co}^{\text{III}}(\text{CN})_6]$.

Introduction

Field-dependent magnetization, $M(H)$, studies are frequently relied upon to ascertain the spin state of a paramagnetic site via fitting the data to the Brillouin function, as was first reported by Henry.¹ This is best established for isolated paramagnetic centers that do not have contributions to the magnetization from orbital angular momentum, spin-orbit coupling, and/or zero-field splitting, as analytical expressions that include these contributions have not been reported. Nonetheless, numerical methods have been developed principally to identify isolated paramagnetic centers present in some proteins.² Likewise, to understand the magnetic couplings (ferro- or antiferromagnetic) and the ground state of molecule-based magnets, $M(H)$ studies are important. In particular we sought to identify the nature of the coupling present in $[\text{Ru}^{\text{II/III}}_2(\text{OAc})_4]_3[\text{Cr}^{\text{III}}(\text{CN})_6]$ ($T_c = 33 \text{ K}$). This magnet possesses $S = 3/2$ $[\text{Ru}^{\text{II/III}}_2(\text{OAc})_4]^+$ and $S = 3/2$ $[\text{Cr}^{\text{III}}(\text{CN})_6]^{3-}$ spin sites;³ however, octahedral Cr^{III} is well modeled by the Brillouin function, and $[\text{Ru}^{\text{II/III}}_2(\text{OAc})_4]^+$ is not.

The physical properties of the mixed-valent, D_{4h} $[\text{Ru}^{\text{II/III}}_2(\text{OAc})_4]^+$ have been extensively studied. This cation has a $\sigma^2\pi^4\delta^2\delta^*\pi^*2$ $S = 3/2$ valence electronic configuration^{4,5} with spins fully delocalized between the two ruthenium centers. However, $[\text{Ru}^{\text{II/III}}_2(\text{OAc})_4]^+$ has an unusually large zero-field splitting (ZFS), D ($+63 \pm 11 \text{ cm}^{-1}$; $D/k_B = 90.6 \pm 15.8 \text{ K}$).^{5–7} $[\text{Ru}^{\text{II/III}}_2(\text{OAc})_4]_3[\text{Cr}^{\text{III}}(\text{CN})_6]$ has $D = 69.4 \text{ cm}^{-1}$ ($D/k_B = 100 \text{ K}$); hence, at low temperature ($\leq T_c$) only the $m_s = 1/2$ state is significantly populated, complicating the analysis of the field-dependent magnetization, $M(H)$ including an anomalous hysteresis loop.³ Due to the presence of zero-field splitting, the Brillouin function cannot be used to model the $M(H)$ data. Nonetheless, there are analytical models for anisotropic temperature-dependent magnetization, $M(T,D)$,^{6a} and herein we extend the methodology used to derive analytical expressions for $M(T,D)$ to derive expressions for $M(H,D)$, and the derived expressions are used to fit the observed $M(H)$ data for $[\text{Ru}_2(\text{OAc})_4]\text{Cl}$ and $[\text{Ru}_2(\text{OAc})_4]_3[\text{Co}(\text{CN})_6]$ with excellent agreement.

Experimental Section

$[\text{Ru}_2(\text{OAc})_4]\text{Cl}$, **1**, and $[\text{Ru}_2(\text{OAc})_4]_3[\text{Co}(\text{CN})_6]$, **2**, were prepared as previously described.³ Field-dependent magnetization measurements were carried out on either a Quantum Design MPMS-5XL SQUID magnetometer from 0 to 5 T or a Quantum Design PPMS Model 9 T susceptometer from 0 to 7.4 T at 2 K as previously described.⁸

Results and Discussion

At 2 K the $M(H)$ of **1** and **2** were observed to be 10 270 and 10 262 $\text{emu}\cdot\text{Oe Ru}_2\text{-eq}^{-1}$ at 5 T, respectively (Figure 1). These values are lower than predicted from the Brillouin function, eq 1 for $S = 3/2$ (i.e., 16 755 $\text{emu}\cdot\text{Oe mol}^{-1}$) due, as discussed above, to the extremely large ZFS of $[\text{Ru}_2(\text{OAc})_4]^+$ ^{5–7} that depopulates the $m_s = 3/2$ energy level at 2 K.⁹ Thus, the only populated state is $m_s = 1/2$. This is in contrast to a 1:1 state occupation for the $m_s = 3/2$ and $m_s = 1/2$ states when the system is isotropic, i.e., $D = 0$. Hence, data were fit to the Brillouin function for $S = 1/2$ that includes a term to account for intradimer interactions θ .¹⁰

$$M(H,\theta)_{\text{Brillouin}} =$$

$$Ng\mu_B S \left[(2S+1) \coth\left(\frac{g\mu_B SH}{k_B(T-\theta)} \frac{2S+1}{2S}\right) - \coth\left(\frac{g\mu_B SH}{k_B(T-\theta)} \frac{1}{2S}\right) \right] \frac{1}{2S} \quad (1)$$

where N is Avogadro's number, g is the Landé factor, μ_B is the Bohr magneton, S is the spin quantum number, and H is the magnetic field, with $g = 3.69$, $\theta = -0.35 \text{ K}$ for **1**, and $g = 3.69$, $\theta = -0.12 \text{ K}$ and for **2** (Figure 1). The small θ values indicate very weak intradimer antiferromagnetic coupling. Weaker coupling is expected via the three diamagnetic five-atom $-\text{NCCo}^{\text{III}}\text{CN}-$ bridges for **2** with respect to the diamagnetic single-atom Cl^- bridge for **1**, as observed.

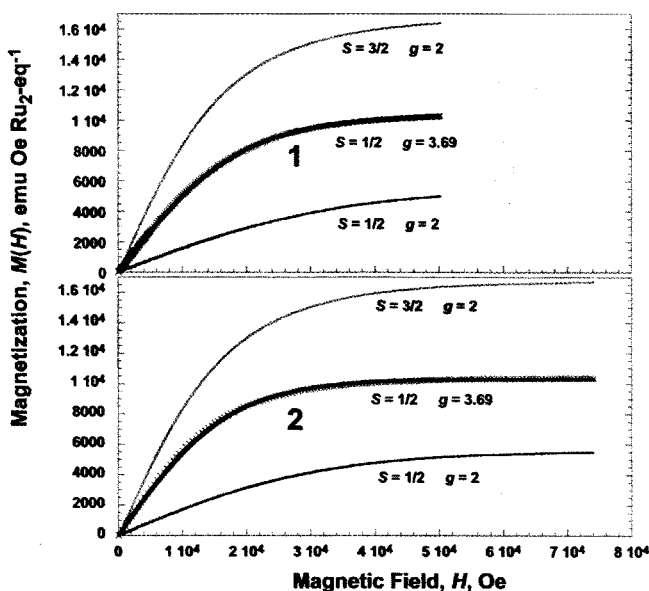


Figure 1. $S = 1/2$ Brillouin function fit, eq 1, with the data of **1** ($S = 1/2$, $g = 3.69$, $\theta = -0.35$ K), and **2** ($S = 1/2$, $g = 3.69$, $\theta = -0.12$ K). The calculated $M(H)$ for $g = 2$, $S = 1/2$, and $S = 3/2$ from eq 1 are shown for comparison. The observed data are plotted as x 's.

The large unphysical 3.69 g -value fit to the Brillouin function emphasizes the inappropriateness of eq 1, which is attributed to the different splitting magnitudes of the $m_s = 1/2$ states arising from the ZFS. The Zeeman splitting used to derive the Brillouin function is $E = \pm g\mu_B H/2$ for $S = 1/2$ but is not valid due to ZFS. Taking into account the anisotropy arising from the ZFS, the splitting for $m_s = 1/2$ is $E_{\parallel} = \pm g_{\parallel}\mu_B H/2$, and $E_{\perp} = \pm g_{\perp}\mu_B H/2 - 3g_{\perp}^2\mu_B^2 H_{\perp}^2/(8D)$,^{11a} Figure 2. Since $\mu_B = 9.274 \times 10^{-24}$ J T^{-1} is small, the latter term for E_{\perp} is negligible. Hence, the perpendicular splitting is twice that of the parallel for $M(H, D)$, thus $g_{M(H, D)\perp} = 2g_{M(H, D)\parallel}$. Given that the Brillouin function is isotropic, $g_{\text{Brillouin}} = g_{\text{Brillouin}\perp} = g_{\text{Brillouin}\parallel}$. The average g value for $M(H, D)$ is $g_{M(H, D)}$ where $g_{M(H, D)} = (2g_{M(H, D)\perp} + g_{M(H, D)\parallel})/3 = (5g_{M(H, D)\parallel})/3$. g_{\parallel} for the Brillouin and $M(H, D)$ expressions are the same, i.e., $g_{M(H, D)\parallel} = g_{\text{Brillouin}\parallel} = g_{\text{Brillouin}} = \pm g_{\parallel}\mu_B H/2$. Thus, $g_{M(H, D)} = (5/3)g_{\text{Brillouin}} = 2.2$; hence, an alternative model is required. Consequently, we sought to fit the data with an analytical expression for $M(H, D, \theta)$.

Analytical expressions for $M(H, D, \theta)$ are not readily available, but numerical methods have been used.^{12a} The $M(H, D)$ calculation by numerical methods takes into account the integration over all space. The integration ensures that all orientations of the sample are included,^{12b} but analytical expressions for this have not been reported. Nonetheless, the structure of diruthenium complex is 3-D body centered, interpenetrating cubic lattice, and the orientation of the crystal at all directions are equivalent, and consequently an analytical expression for $M(H, D, \theta)$ was derived.

Analytical Expression for $M(H, D, \theta)$. $[\text{Ru}_2(\text{OAc})_4]^+$ possesses an $^4B_{2u}$ ground state and $^2A_{1u}$, $^2A_{2u}$, $^2B_{2u}$, $^2B_{1u}$ excited states; however, the excited states do not contribute to the paramagnetism.^{5b} Thus, the excited states are neglected. In the case of isotropic $S = 3/2$, both the $m_s = \pm 3/2$ and $\pm 1/2$ energy levels are essentially equally populated. These states, however, are not evenly populated due to the ZFS, D , arising from the tetragonal distortion, and the larger the $|D|$, the greater the difference in the population of the states, especially for $T \approx |D|$. The ZFS Hamiltonian, \hat{H}_{ZFS} , in an octahedral crystal field with Zeeman effect is used to describe this phenomenon.

$$\hat{H}_{\text{ZFS}} = g\mu_B \hat{S} \cdot \underline{H} + D \left[\hat{S}_z^2 - \frac{S(S+1)}{3} \right] + E(\hat{S}_x^2 - \hat{S}_y^2) \quad (2)$$

where D is the axial ZFS tensor, E is the rhombic ZFS tensor, S_z is the spin at parallel direction with respect to H , while S_x and S_y are the spins perpendicular with respect to H . Since there is no rhombic distortion in the system (i.e., $E = 0$),⁶ the Hamiltonian reduces to:

$$\hat{H}_{\text{ZFS}} = g\mu_B \hat{S}_z \cdot H_z + g_x \mu_B \hat{S}_x \cdot H_x + g_y \mu_B \hat{S}_y \cdot H_y + D \left[\hat{S}_z^2 - \frac{S(S+1)}{3} \right] \quad (3)$$

and the energy of the ZFS Hamiltonian can be expressed by the secular determinant as:

$$\begin{vmatrix} \langle 1/2 | & \langle -1/2 | & \langle 3/2 | & \langle -3/2 | \\ \langle 1/2 | & 2D + \frac{3}{2}g\mu_B H_z & 0 & \frac{\sqrt{3}}{2}(g\mu_B H_x + ig\mu_B H_y) \\ \langle -1/2 | & 0 & 2D - \frac{3}{2}g\mu_B H_z & \frac{\sqrt{3}}{2}(g\mu_B H_x - ig\mu_B H_y) = E_{\text{ZFS}} \\ \langle 3/2 | & \frac{\sqrt{3}}{2}(g\mu_B H_x - ig\mu_B H_y) & 0 & \frac{1}{2}g\mu_B H_z \\ \langle -3/2 | & 0 & \frac{\sqrt{3}}{2}(g\mu_B H_x + ig\mu_B H_y) & -\frac{1}{2}g\mu_B H_z \end{vmatrix} \quad (4)$$

The anisotropic magnetization function, $M(H, D, \theta)$, for $S = 3/2$ is derived from the ZFS Hamiltonian, eq 3, and magnetization equation. We introduce the Weiss constant, θ , to account for weak intermolecular coupling.^{11b}

$$M(H, D, \theta)_{\parallel} = N \left[3g\mu_B \sinh \left(\frac{3}{2} \frac{g\mu_B H}{k_B(T - \theta)} \right) \exp(-2D/k_B T) + g\mu_B \sinh \left(\frac{g\mu_B H}{2k_B(T - \theta)} \right) \right] \left[2 \cosh \left(\frac{3}{2} \frac{g\mu_B H}{k_B(T - \theta)} \right) \times \exp(-2D/k_B T) + 2 \cosh \left(\frac{g\mu_B H}{2k_B(T - \theta)} \right) \right] \quad (5a)$$

$$M(H, D, \theta)_{\perp} = N \left[\frac{-3}{2D} g^2 \mu_B^2 H \exp \left(\frac{-2D - \left[\frac{3}{8D} g^2 \mu_B^2 H^2 \right]}{k_B T} \right) + \frac{3}{2D} g^2 \mu_B^2 H \cosh \left(\frac{-g\mu_B H}{k_B(T - \theta)} \right) - 2g\mu_B \sinh \left(\frac{-g\mu_B H}{k_B(T - \theta)} \right) \right] \left[2 \exp \left(\frac{-2D - \left[\frac{3}{8D} g^2 \mu_B^2 H^2 \right]}{k_B T} \right) + 2 \cosh \left(\frac{-g\mu_B H}{k_B(T - \theta)} \right) \right] \quad (5b)$$

$$M(H, D, \theta)_{\text{AVERAGE}} = \frac{M(H)_{\parallel} + 2M(H)_{\perp}}{3} \quad (5c)$$

Indeed, using eq 5, $M(H, D, \theta)$ gave the best fit for **1** with $g = 2.253$, $D = 69.4$ cm^{-1} ($D/k_B = 100$ K), and $\theta = -0.56$ K, with a χ^2 agreement factor¹³ = $\sum(M_{\text{observed}} - M_{\text{calc}})^2/M_{\text{observed}}^2 = 1.0046$. The best fit for **2** with $g = 2.235$, $D = 69.4$ cm^{-1}

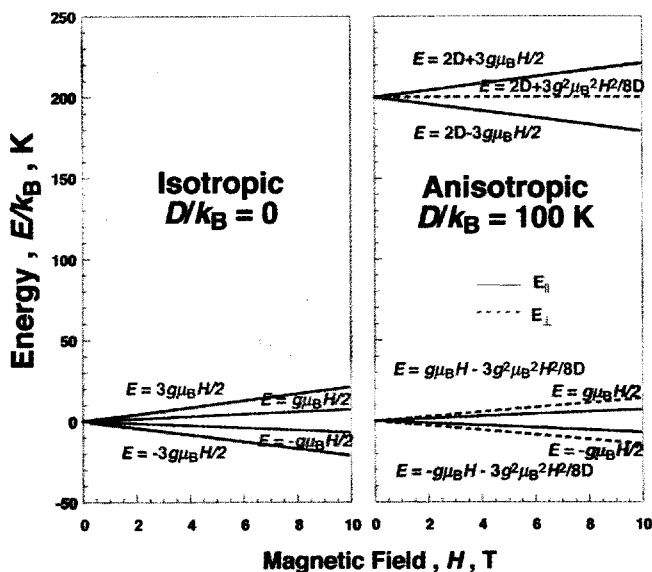


Figure 2. Energy spectra of $S = 3/2$ energy levels with Zeeman effect, and isotropic and anisotropic for $D = 69.4 \text{ cm}^{-1}$ ($D/k_B = 100 \text{ K}$).

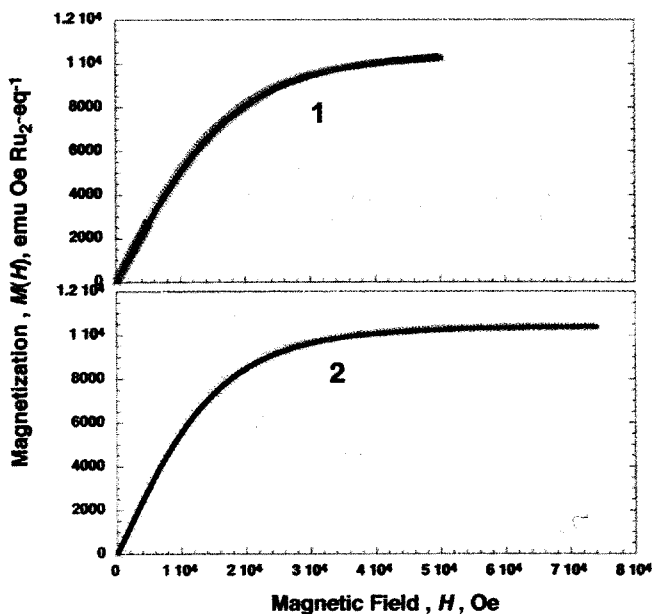


Figure 3. Observed $M(H, D, \theta)$ (\times) for **1** ($g = 2.253$, $D = 69.4 \text{ cm}^{-1}$ ($D/k_B = 100 \text{ K}$), and $\theta = -0.56 \text{ K}$) and **2** ($g = 2.235$, $D = 69.4 \text{ cm}^{-1}$ ($D/k_B = 100 \text{ K}$), $\theta = -0.24 \text{ K}$), and their fits to eq 5.

($D/k_B = 100 \text{ K}$), $\theta = -0.24 \text{ K}$ ($\chi^2 = 0.93$) (Figure 3). Again, the small θ values indicate very weak intradimer antiferromagnetic coupling.

The observed magnetizations $10,270$ and $10,262 \text{ emu}\cdot\text{Oe Ru}_2\text{-eq}^{-1}$ at 5 T for **1** and **2**, respectively, are consistent with only the $m_s = 1/2$ energy level being populated. The observed magnetization is the first plateau, and it should eventually rise to about $18,900 \text{ emu}\cdot\text{Oe Ru}_2\text{-eq}^{-1}$ when saturation occurs. This saturation magnetization is predicted to be the same value as that predicted by the Brillouin function, i.e., $18,880$ and $18,725 \text{ emu}\cdot\text{Oe Ru}_2\text{-eq}^{-1}$ for **1** and **2**, respectively.

Since the anisotropic magnetization function is derived from second-order degenerate perturbation, $|D| \gg g\mu_B H$ was assumed. For large applied magnetic fields, $D \approx g\mu_B H$; hence, second-order perturbation is not valid. Consequently, there will be energy crossing when $D \approx g\mu_B H$, but to fully understand and

to predict this energy-crossing phenomena, which results in the magnetization steps, an exact solution of the Hamiltonian, or higher-order perturbations, is required. This is a focus of ongoing studies, which will predict both energy-crossing and noncrossing effects. The noncrossing energy is due to the noncrossing rule, in which energy from spins that possess the same symmetry does not cross, and as a consequence, the energy-level mixing should occur.

Conclusion

Extension of the classical Brillouin function, $M(H)$, to include zero-field splitting (ZFS), D , [$|D| \gg g\mu_B H$] [and an intermolecular interaction (θ)], to a general analytical expression for the anisotropic magnetization function, $M(H, D, \theta)$, has been derived. This equation describes the unusually low values of the observed magnetization for $[\text{Ru}^{\text{III}}_2(\text{OAc})_4]^+$. Deviations from the classical Brillouin function are a consequence of differing energy levels with respect to the isotropic energy levels used to derive the Brillouin function. However, further theoretical studies and high-field experiments will enable the understanding of the spin behavior upon saturation and energy-level crossover for materials with zero-field splitting.

Acknowledgment. We gratefully acknowledge the partial support from the U.S. DOE (Grant No. DE FG 03-93ER45504), the Air Force Office of Scientific Research (Grant No. F49620-00-1-0055), and the ACS PRF (Grant No. 36165-AC5).

References and Notes

- (1) Henry, W. E. *Phys. Rev.* **1952**, *88*, 559.
- (2) Day, E. P. *Methods Enzymol.* **1993**, *227*, 437.
- (3) Liao, Y.; Shum, W. W.; Miller, J. S. *J. Am. Chem. Soc.* **2002**, *124*, 9336.
- (4) Cotton, F. A.; Walton, R. A. *Multiple Bonds between Metal Atoms*, 2nd ed.; Clarendon Press: Oxford, UK, 1993; p 18.
- (5) (a) Norman, J. G., Jr.; Renzoni, G. E.; Case, D. A. *J. Am. Chem. Soc.* **1979**, *101*, 5256. (b) Miskowski, V. M.; Hopkins, M. D.; Winkler, J. R.; Gray, H. B. In *Inorganic Electronic Structure and Spectroscopy*; Solomon, E. I., Lever, A. B. P., Eds.; John Wiley & Sons: 1999; Vol. 2, Chapter 6.
- (6) (a) Telser, J.; Drago, R. S. *Inorg. Chem.* **1984**, *23*, 3114. Cukiernik, F. D.; Giroud-Godquin, A. M.; Maldivi, P.; Marchon, J. C. *Inorg. Chim. Acta* **1994**, *215*, 203. Handa, M.; Sayama, Y.; Mikuriya, M.; Nukada, R.; Hiromitsu, I.; Kasuga, K. *Bull. Chem. Soc. Jpn.* **1998**, *71*, 119. Jimenez-Aparicio, R.; Urbanos, F. A.; Arrieta, J. M. *Inorg. Chem.* **2001**, *40*, 613.
- (7) Cukiernik, F. D.; Luneau, D.; Marchon, J. C.; Maldivi, P. *Inorg. Chem.* **1998**, *37*, 3698.
- (8) Brandon, E. J.; Rittenberg, D. K.; Arif, A. M.; Miller, J. S. *Inorg. Chem.* **1998**, *37*, 3376.
- (9) $\exp(-2D/k_B T) = 3.72 \times 10^{-44} \approx 0$ (unitless), for $D/k_B = 100 \text{ K}$, and $k_B = 1.38 \times 10^{-23} \text{ J/K}$.
- (10) Deakin, L.; Arif, A. M.; Miller, J. S. *Inorg. Chem.* **1999**, *38*, 5072.
- (11) Kahn, O. *Molecular Magnetism*; VCH Publishers: New York, NY, 1993. (a) p 23. (b) p 5.
- (12) (a) Shapira, Y.; Bindilatti, V. *Appl. Phys. Rev.* **2002**, *92*, 4155. Boskovic, C.; Wernsdorfer, W.; Foltling, K.; Huffman, J. C.; Hendrickson, D. N.; Christou, G. *Inorg. Chem.* **2002**, *41*, 5107. Brechin, E. K.; Boskovic, C.; Wernsdorfer, W.; Yoo, J.; Yamaguchi, A.; Sanudo, E. C.; Concolino, T. R.; Rheingold, A. L.; Ishimoto, H.; Hendrickson, D. N.; Christou, G. *J. Am. Chem. Soc.* **2002**, *124*, 9710. Gonzalez, R.; Chiozzone, R.; Kremer, C.; De Munno, G.; Nicolo, F.; Lloret, F.; Julve, M.; Faus, J. *Inorg. Chem.* **2003**, *42*, 2512. The attempt to reproduce the same calculation in the article by the parameters reported did not give us a satisfying result. An alternative using eq 5 with the best-fit parameters, $g = 3.25$, $M(H, D, \theta)$ with $|D| = 24.3 \text{ cm}^{-1}$ as reported to model the data gave us $g = 1.98$ and $\theta = -0.2 \text{ K}$. (b) Vincent, J. B.; Christmas, C.; Chang, H.; Li, Q.; Boyd, P. D. W.; Huffman, J. C.; Hendrickson, D. N.; Christou, G. *J. Am. Chem. Soc.* **1989**, *111*, 2086. Vermaas, A.; Groeneveld, W. L. *Chem. Phys. Lett.* **1974**, *27*, 583.
- (13) Taylor, J. *An Introduction to Error Analysis*; University Science Books: Mill Valley, CA, 1982; pp 218–223.